Eur. Phys. J. E (2012) **35**: 105
DOI 10.1140/epje/i2012-12105-y

THE EUROPEAN PHYSICAL JOURNAL E

Regular Article

Stuck in traffic: Patterns of powder adhesion*

N. Nirmal Thyagu[1], A. Vasilenko[2], A. Voyiadjis[1], B.J. Glasser[2], and T. Shinbrot[1,a]

[1] Department of Biomedical Engineering, Rutgers University, Piscataway, NJ 08854, USA
[2] Department of Chemical & Biochemical Engineering, Rutgers University, Piscataway, NJ 08854, USA

Received 12 July 2012 and Received in final form 3 September 2012
Published online: 22 October 2012 –

Abstract. The adhesion of fine particles to surfaces is important for applications ranging from drug delivery to fouling of solar cells. In this letter, we show that powder adhesion can occur in unexpected patterns, concentrating particular grain types in some locations and clearing them from others, and we propose a straightforward traffic model that appears to reproduce many of the behaviors seen. The model predicts different patterns depending on inter-particle cohesion, and we find in both experiment and model that adhesion occurs in three distinct stages.

Particle adhesion limits the size of micropatterned circuits [1], the effectiveness of inhaled medicines [2], and causes significant downtime in pharmaceutical tableting [3] and food processing [4] operations. Likewise, the lifetime of photoelectric cells on Mars Exploration Rovers has been tied to dust accumulation on their surfaces [5,6], and abrasion by adhered dust is a recognized limitation on extraterrestrial exploration [7–9]. An example of powder adhesion patterns is shown in fig. 1(a), where we display the inside of a tumbler after it has been used to mix a blend of common pharmaceuticals containing 25% by mass acetaminophen (APAP) and 75% lactose, a standard excipient. The inset to fig. 1(a) shows the tumbler used: a stainless steel "V-blender", which is one of the mainstays of powder mixing [10,11]. This blender is a 16 qt. capacity tumbler consisting of two cylinders joined together at 90° and tumbled about the axis shown in the inset. Figures 1(b)-(c) show successive enlargements of adhered powder: in panel (c) it is evident that much of the powder consists of elongated particles, characteristic of the active ingredient [12] used in this blend, but not of the inactive excipient [13] with which it is mixed. Figure 1(d) confirms this finding: in this panel, we show the UV spectroscopic analysis of adhered grains scraped from the tumbler walls. Evidently as time elapses, the concentration of active material adhered grows to about double that in the bulk, thus the phenomenon of powder sticking has significant practical repercussions as it affects drug concentrations both in the bulk —leading to subtherapeutic medications— and in adhered chunks (cf. fig. 4(a)) that can break off, yielding superpotent dosages.

Apparently, the sticking of powder to processing surfaces leads to two unexpected behaviors: spontaneous formation of striped adhesion patterns and preferential concentration of particular powder types in the adhered material. Notwithstanding prior work in this field [14], neither of these behaviors appears to have been reported before, and both are unexplained.

In the present work, we seek to elucidate the mechanism for the first behavior, patterning, leaving analysis of increased concentration for future study. We start by describing the time progression of the patterns shown in fig. 1, then we describe a model that contains the essential elements known to be present in the physical problem, and finally we challenge the model under atypical conditions and evaluate whether it correctly predicts qualitative changes in pattern formation seen in experiments.

In fig. 2, we show a typical time progression, tumbling a half-full blender through 5, 15, 100, and 300 revolutions at 25 rpm. In the top panels of the figure, we show the view through the bottom opening of the tumbler (at the apex of the "V"), with location identified in the inset to the lower panel. The bottom seal can be released smoothly with minimal disturbance to powder on the tumbler surface, and this viewpoint affords a clear image of the patterns with minimal anisotropy. Figure 2 is typical of the patterning behaviors that we see in multiple trials, and consists of three distinct stages. First, the surface of the tumbler is nearly uniformly dusted with powder (fig. 2(a)); next, the powder is cleared from some regions (*e.g.* within red circle in fig. 1(b)), which are black in the snapshots, and deposited in others, which are white (fig. 2(b)-(c)). Finally, as powder is increasingly deposited onto the surface, the powder-free regions contract. We can quantify this process

* Supplementary material in the form of 3 .mov files and a .txt file available from the Journal web page at
http://dx.doi.org/10.1140/epje/i2012-12105-y

[a] e-mail: shinbrot@rutgers.edu

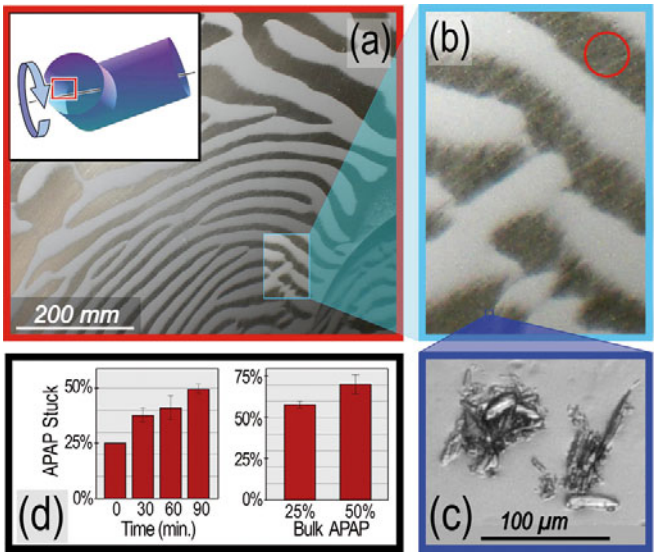

Fig. 1. Pharmaceutical powder adhered to tumbler after emptying, exhibiting preferential attachment of active ingredient to striped patterns. Tumbler is stainless steel, filled 50-60% by volume with a 50/50 mixture of acetaminophen (APAP) and excipient (here lactose), and tumbled 30 minutes at 25 rpm. (a) Overview of adhered pattern; inset shows the tumbler used, where the red box is the location of the main plot. (b) Enlargement of pattern. Mean flow here is from upper right to lower left: note that the stripes are transverse to the flow direction. Areas nearly free of powder (red circle) show the surface texture: 180 grit 2G sanitary finish. (c) Micrograph of adhered particles, showing crystalline structure characteristic of APAP: snapshot taken by lifting powder from the surface with sticky tape and imaging with Olympus IX81 inverted microscope. (d) Concentrations of APAP in adhered powder scraped from tumbler surface after tumbling for 30 minutes and emptying tumbler. Separate experiments are performed for each data point shown, beginning with fresh powder. Left plot shows time progression of APAP concentration scraped from tumbler walls, using 25/75 blend of APAP (micronized, from Mallinckrodt Inc.) and microcrystalline cellulose (MCC: Avicel® PH 101 from FMC Inc.) excipient. Averages are over 9 samples at times 30 and 90; 6 samples at time 60. Right plot shows APAP concentrations in blends with 25% and 50% bulk concentration of APAP tumbled with MCC for 30 minutes at 25 rpm; averages are over 5 samples in each case. At 25%, data are obtained using UV spectroscopy; at 50%, IR spectroscopy is used. Error bars are standard errors.

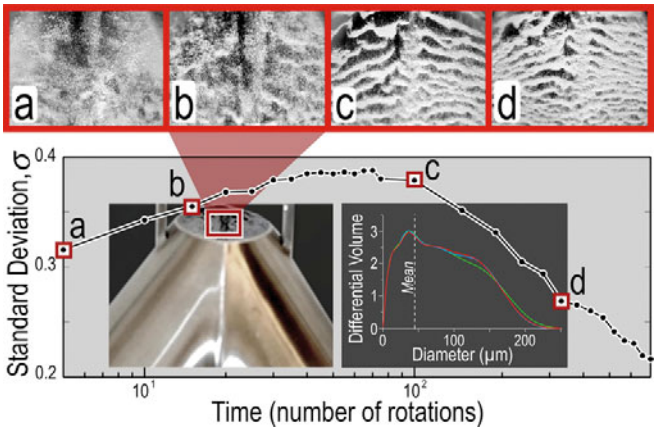

Fig. 2. (a)-(d) Experimental progression of adhered patterns inside V-blender, tumbling at 15 rpm and RH 45%. Lower panel: Standard deviation of grayscale as a function of time, showing a maximum at about 100 rotations. Left inset: location of snapshots, at bottom opening of tumbler. Right inset: particle sizes, measured for three samples using laser diffraction (Beckman Coulter, model LS 13 320 particle size analyzer in dry powder mode using Tornado Powder attachment). Mean particle size shown is 45 μm.

by measuring the standard deviation, σ, of the grayscale, as shown in the lower panel of fig. 2. σ has the useful property of being larger when stronger gradients between white and black regions are present, and smaller when the surface is more uniform. As we have described qualitatively, initially and finally the surface is nearly uniform —hence σ is smaller— and at intermediate times, sharply defined patterns are seen —hence σ is larger.

Thus, to understand the patterning behaviors in sticking powders, we must explain all three stages described above: 1) why uniform dusting occurs, 2) why powder-free regions emerge between dense stripes of adhered powder, and 3) how the surface becomes more uniformly covered again. Before we model these processes, we note that the flow dynamics in the V-blender are notoriously complex, with powder sloshing from center to arms of the V and back [15], flowing more smoothly from leading to trailing side [10], and being complicated by left-right diffusive [16] as well as segregational [17] transport. Modeling these global complexities would be a dubious undertaking; moreover, the patterning seen evidently covers the entire interior of the tumbler, irrespective of regional differences in flow. Therefore we focus on what occurs locally, at all regions of the surface.

Locally speaking then, three fundamental processes are known to occur at the surface. First, powder is deposited on the surface [18] during repeated contacts with the powder bed. Second, erosion is known to remove powder from surfaces [19] through these same contacts. Third, friction with the bed on the surface causes adhered powder to be advected in an average streamwise direction [20].

We include these processes in a simulation by defining a surface on which we add and erode particles at fixed rates, and allowing particles at the surface to be transported in a streamwise direction. As we will describe, streamwise transport consists of a simple traffic model, obeying a prescribed rule that makes use of current understanding of granular dynamics. In detail, the model that we use is 2D, representing the tumbler surface, and for simplicity is periodic from -5 to 5 in both x and y. We model 1) particle accretion, 2) erosion and 3) transport as follows.

1) To model particle accretion, every computational timestep, a fixed number, N_{add}, of point particles are added at random locations. In the simulations shown below, we use a Gaussian distribution of initial particle locations, centered at the origin, and with standard devi-

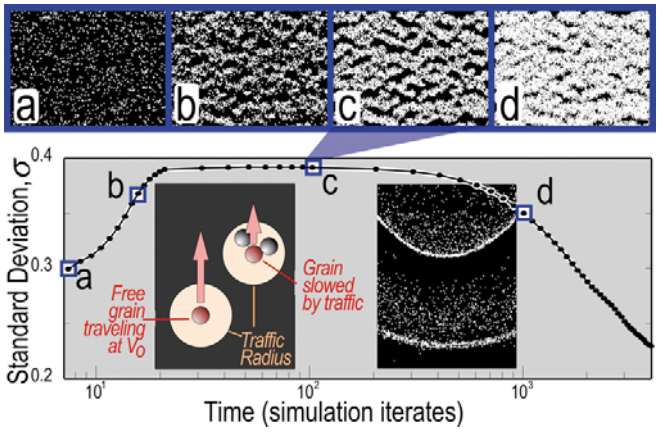

Fig. 3. (a)-(d) Computational progression of patterns on a periodic surface. Movies of the evolution along with code used in the simulations are included in the supplementary material to this paper. Lower panel: standard deviation of grayscale as a function of time, showing a maximum at about 100 rotations. Left inset: schematic of simulation described in text, showing that adhered convoys of particles are slowed in proportion to number of neighbors as in eq. (1). Right inset: sharpening of leading edge and feathering of trailing edge of stripes described in text.

ations, $\sigma_x = \sigma_y = 0.7$. The use of a Gaussian distribution is motivated by the fact that diffusing particles will ultimately adopt a Gaussian, so starting them off this way should limit initial transients; comparison simulations using uniform or other particle distributions exhibit similar asymptotic patterns. We have investigated numerous choices of $N_{\rm add}$; increasing $N_{\rm add}$ chiefly reduces the timescale before the surface becomes completely covered, but has little effect on the patterns produced. We show $N_{\rm add} = 300$ below.

2) To model erosion of adhered particles by the overlying bed, we remove a fixed number, $N_{\rm erode}$, particles chosen at random from the surface. Again, numerous choices were investigated; the ratio between $N_{\rm erode}$ and $N_{\rm add}$ governs the net rate of surface coverage, but has little other qualitative effect on the patterns expressed. We show $N_{\rm erode} = 10$ below.

3) Finally, to model transport, we define particles at the surface to travel in the streamwise direction at a speed determined by the number of nearby neighbors. That is, as depicted in the lower left inset to fig. 3, we assume that a single particle will find it difficult to adhere the surface by itself and so will travel at the speed of the overlying bed flow, but once other particles have adhered, a new particle will exhibit a greater tendency to stick. This is a universal feature of sticking, undergirding everything from the need to brush teeth regularly [21] to the kinetics of coating processes [22]. Explicitly, particles move in the y-direction at speed V_y defined by:

$$V_y = V_0 \cdot \max\left[0, \left(1 - \frac{N}{N_c}\right)\right], \qquad (1)$$

where V_0 is the speed of an isolated particle produced by the ambient tumbling flow, and N_c is the number of neighboring particles with centers within a "traffic radius" R_c that cause the given particle to come to a halt. We use $V_0 = 0.5$, $N_c = 10$, and $R_c = 0.2$ in fig. 3.

As depicted in the schematic of fig. 3, eq. (1) prescribes that isolated particles travel at speed V_0, and convoys of cohesive particles travel at a monotonically decreasing speed that jam when a critical density, $\rho_c = N_c/\pi R_c^2$, is reached, cf. refs. [23,24]. This model is in a tradition of granular traffic models [25,26]: every particle acts as a vehicle in traffic, traveling with fixed maximum speed V_0 on an empty roadway, and decreasing in speed with the number of neighbors until a critical density is reached at which a jam occurs. We note that this model represents a 2D projection of a 3D pattern as has also been used before [27], so particles have no fixed radius, but are point-like and can overlap on the projected plane.

We discuss effects of parameter variations shortly; for the time being, we use this traffic model to produce the time series of snapshots shown in the top panels of fig. 3. We find that initially the 2D domain is uniformly dusted with particles (fig. 3(a)), which thereafter are swept forward at speed V_0 until they produce denser convoys of slower moving neighbors (figs. 3(b)-(c)), separated from one another by nearly empty surface regions. This produces a growth in the standard deviation at intermediate times shown in the lower panel of fig. 3 and seen also in experiment. We define $N_{\rm add} > N_{\rm erode}$, so that more particles adhere than are eroded, causing the surface to fill over longer times, again as seen in experiment.

We remark that this model has the incidental feature that at the boundaries of each convoy, particles have fewer neighbors than within, and these particles can accelerate to either compactify the convoy (at the rear) or spread (at the front) as is seen in experiments (*e.g.*, fig. 1(b)). This contrast between leading and trailing edges of stripes is well known in the study of shocks in traffic, but is not evident at the low resolution of the snapshots of fig. 3. Moreover, the random addition of particles over time tends to blur stripe boundaries. Since the contrast can be seen at high resolution, *e.g.* fig. 1(b), we challenged the simulation by distributing a large number of particles (32000) uniformly over a small domain (1×1 units). As shown in the lower right inset to fig. 3, the expected sharp leading edge appears, here after 40 timesteps without erosion or deposition of particles and using $V_0 = 0.05$, $N_c = 6400$, and $R_c = 0.1$.

As a final challenge to the model, we compare its results with experiments that we have performed under different environmental conditions, at different fill levels and tumbling speeds, in different size tumblers, and using different concentration powders. We find from these experiments that striped patterns invariably form, provided that the relative humidity is in a range between 40 and 60%, and the tumbler surface is sufficiently clean and rough that an initial layer can take hold. Thus, for example, if the surface is contaminated with fused silica (a common glidant that makes the surface slippery), the formation of patterns is significantly inhibited, however cleaning with

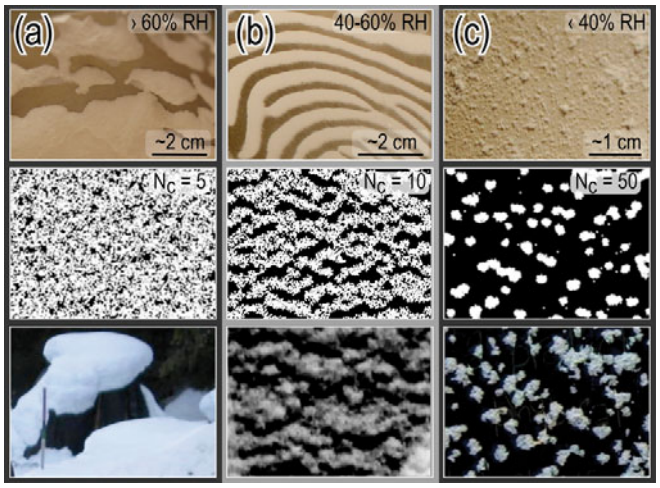

Fig. 4. Patterns in adhered powders seen in simulations and experiments. Upper panels: pattern transition from clumps to stripes to spots seen on tumbler surface, as relative humidity (RH) is decreased. In leftmost example, at high RH, 20 grams adhere to the surfaces after the tumbler has been emptied; by contrast in the other cases, about 2 grams typically adhere. In all cases, powder shown and weighed remains adhered after emptying tumbler and repeatedly striking it forcefully. Blenders in panels (a) and (b) are tumbled at 25 rpm for 15 and 30 minutes respectively. Panel (c) is tumbled at 15 rpm for 20 minutes. All panels show V-blender filled to about 50% by volume, and scale bars are approximate. Central panels: computational transitions seen as the critical number, N_c, of particles needed within a radius $R_c = 0.2$ to make a cluster jam is increased. Lower panels: patterns seen in windblown snow (left) and snow on nearly black sandwich boards (latter two images: contrast enhanced, figure credits due to Justin Kao).

a solvent such as acetone restores the sticking behavior. In fig. 4, we show changes in adhesion patterns that appear across a range of relative humidity (RH). In each experiment, we acclimatize the powders and the tumbler at constant humidity for at least a day beforehand.

Evidently in both experiment and simulation, three patterned states can emerge. 1) If particles are strongly cohesive (*i.e.* at high humidity, RH, or small number of particles required to cause a jam, N_c) aggregates grow to cover the available surface. 2) If particles are moderately cohesive (intermediate RH or N_c), jams form in the streamwise direction and coordinate spanwise to form stripes. And 3), for weak particle cohesion (small RH or large N_c), spanwise growth cannot be sustained, and only rounded spots form. We theorize that spots are produced because this state maximizes the number of particles (and so the aggregate cohesion) per unit area. In the model, this leads to the promotion of localized jamming, and equivalently in experiments, this increases the total stress available to hold the aggregate in place. We note that the mechanism leading to pattern choice provides a diagnostic for underlying cohesion strengths —that is, uniform coverage or stripe formation in an experiment is indicative of comparatively strong cohesion, while the formation of spots is indicative of a less cohesive powder.

In conclusion, we have shown that powders adhere to processing surfaces in complex patterns. A simple traffic model appears to capture many of the patterning behaviors seen, including stripe formation, clearing of surfaces between stripes, sharpening lead edges of the stripes, and stripe-spot transitions. The formation of stripes of particulates stuck to surfaces has been reported for other systems as well, for example in dip-coated colloids [24,28] and in biofilm development [29,30]. Therefore we speculate that similar processes may be at work in the adhesion of other types of particles to surfaces —for example as insets to the lower panels of fig. 4 we show snow that has adhered, left to right, to a large boulder, and to two wooden sandwich-boards outside of Boston restaurants. It remains for future studies to establish why particular materials tend to preferentially occupy the adhered powder layers, and what properties of surfaces may promote or inhibit adhesion patterns.

We thank Justin Kao and Peko Hosoi for helpful discussions, and Jihyung Chun, Ankur Patel, Francis Romanski, and Aditya Vanarase for technical support. This work was partially supported by the National Science Foundation.

References

1. O. Gefen, N.Q. Balaban, Trends Biotechnol. **26**, 345 (2008).
2. E.A. Matida, W.H. Finlay, C.F. Lange, B. Grgic, J. Aerosol Sci. **35**, 1 (2004).
3. J.J. Wang, T. Li, S.D. Bateman, R. Erck, K.R. Morris, J. Pharm Sci. **92**, 798 (2003).
4. L. Ahrné, A. Chamayou, K. Dewettinck, F. Depypere, E. Dumoulin, J. Fitzpatrick, G. Meesters, in *Food Materials Science: Principles and Practice*, edited by J.M. Aguilera, P.J. Lillford (Springer, 2008).
5. G.A. Landis, *Proceedings of Energy Conversion Engineering Conference* (Honolulu, 1997).
6. D.D. Sentman, *Sand and Dust on Mars*, edited by R. Greeley, R.M. Haberle (NASA, Ames Research Center, 1991) p. 53.
7. D. Mackenzie, New Scientist **2501**, 40 (2005).
8. L.V. Starukhina, Lunar Plan. Sci. **XXXVI**, 1343 (2005).
9. D.C. Ferguson, J.C. Kolecki, M.W. Siebert, D.M. Wilt, J.R. Matijevic, J. Geophys. Res. **104**, 8747 (1999).
10. M. Moakher, T. Shinbrot, F.J. Muzzio, Powder Technol. **109**, 58 (2000).
11. T. Shinbrot, F.J. Muzzio, *Mixing and segregation in tumbling blenders*, in *Encyclopedia of Pharmaceutical Technology* (Marcel-Dekker, 2002) pp. 1805-20.
12. T. Lee, C.S. Kuo, Y.H. Chen, Pharma. Technol. **30**, 72 (2006).
13. P. Narayan, B.C. Hancock, Mat. Sci. Eng. A **355**, 24 (2003).
14. S.W. Booth, J.M. Newton, J. Pharm. Pharmacol. **39**, 679 (1987).
15. J.P. Kuo, P.C. Knight, D.J. Parker, Y. Tsuji, M.J. Adams, J.P.K. Seville, Chem. Eng. Sci. **57**, 3621 (2002).
16. D. Brone, C. Wightman, K. Connor, A.W. Alexander, F.J. Muzzio, P. Robinson, Powder Technol. **91**, 165 (1997).

17. A.W. Alexander, T. Shinbrot, B. Johnson, F.J. Muzzio, Int. J. Pharm. **269**, 19 (2004).
18. A.D. Zimon, *Adhesion of dust and powder* (Plenum Press, New York, 1982).
19. I. Kleis, P. Kuly, in *Solid Particle Erosion, Occurrence, Prediction and Control* (Springer-Verlag, London, 2010) pp. 129-168.
20. R.D. Amell, *Tribology: principles and design applications* (MacMillan, New York, 1991) pp. 91-92.
21. B. Rosan, R.J. Lamont, Microbes, Infect. **2**, 1599 (2000).
22. T.D. Dabros, T.G.M. Van de Ven, J. Colloid Interface Sci. **89**, 232 (1982).
23. V. Trappe, V. Prasad, L. Cipelletti, P.N. Segre, D.A. Weitz, Nature **411**, 772 (2001).
24. J.C.T. Kao, A.E. Hosoi, Phys. Fluids **24**, 041701 (2012).
25. D.E. Wolf, M. Schreckenberg, A. Bachem (Editors), *Traffic and Granular Flow* (World Scientific, Singapore, 1996).
26. Y. Sugiyama, M. Fukui, M. Kikuchi, K. Hasebe, A. Nakayama, K. Nishinari, S. Tadaki, S. Yukawa, New J. Phys. **10**, 033001 (2008).
27. T. Shinbrot, Nature **389**, 574 (1997).
28. M. Ghosh, F.Q. Fan, K.J. Stebe, Langmuir **23**, 2180 (2007).
29. C.M.L. Bollen, M. Quirynen, J. Clin. Periodont. **22**, 1 (1995).
30. K. Agladze, D. Jackson, T. Romeo, J. Bacteriol. **185**, 5632 (2003).